Computed Tomographic Scanning in Children: Comparison of Radiation Dose and Resolving Power of Commercial CT Scanners

ROBERT C. BRASCH,[1] DOUGLAS P. BOYD, AND CHARLES A. GOODING

Surface and internal radiation doses for abdominal computed tomography (CT) of children were determined using child-sized phantoms and seven models of CT body scanners. Resolving power of each scanner was determined simultaneously with the radiation dose determination. The average surface skin dose for a complete CT body examination ranged from 0.39 to 5.60 rad, varying with patient size and model of CT scanner employed. A high contrast (12%) resolving power phantom of water-filled holes in acrylic showed a range of 1.75–2.25 mm.

Introduction

Knowledge of patient radiation dose received from computed tomography (CT) with whole body scanners is essential to the determination of a benefit-risk ratio for this procedure. The radiation dose to children, for whom dose is perhaps most important, has not been determined. Information on radiation exposure is essential to both the clinician requesting a CT examination and the radiologist performing these examinations. Heretofore, an independent study of dose from different models of CT body scanners performed with the same phantom or phantoms under similar circumstances has not been available. The purpose of this study was to determine the range of patient radiation dose for CT body examinations of children with clinically employed CT techniques using several commercial CT body scanners.

Two specially constructed plastic phantoms, one resembling the size of a 10-year-old child's abdomen and the other resembling a 6-month-old infant's abdomen, were scanned in each scanner. Surface and internal radiation doses were determined with thermoluminescent dosimeters fitted around and within the phantoms. Resolving power was simultaneously determined with a series of variable-sized water-filled holes in acrylic within the phantoms. The axial dose distribution of a single CT section was measured for each scanner because this is one important determinant of the total radiation dose from a complete CT examination of several CT sections. Determinations were made with the following CT body scanners: EMI-Tronics CT 5005, General Electric CT/T, Ohio Nuclear Delta 50, Ohio Nuclear Delta fast scanner, Ohio Nuclear Delta 2000 preproduction prototype, Pfizer 200 FS, and the Varian CT scanner.

Materials and Methods

Dosimeters

Radiation dose determinations were made with commercially available thermoluminescent dosimeters (Radiation Detection Co., Sunnyvale, Calif.). The dosimeter capsules were 15 mm long and 3 mm in diameter allowing insertion into holes perpendicular to the tomographic section within the plastic phantoms. The final radiation dose readings were provided by the supplier with a reported precision of ±10% for doses over 100 mR. The dosimeters were calibrated for radiation doses less than 100 rad in the range of diagnostic x-ray energies.

Phantoms

Two phantoms (fig. 1) made in sections of polystyrene and acrylic were constructed to simulate the sizes and abdominal contours of a 6-month-old infant and a 10-year-old. The circumference of the smaller phantom was 36 cm and that of the larger phantom was 66 cm. Narrow grooves, designed to hold dosimeter capsules, were placed on the anterior, posterior, and lateral aspects of the central section of each phantom. Within the central section, holes were drilled in the center and in each of the four quadrants. An additional dosimeter capsule could be fitted to the end of a plastic rod which extended 32 cm from the central section. The dose recorded at the end of the rod was intended to simulate the dose to the thyroid gland. In total, 10 dosimeter capsules (four circumferential, five internal, and one "thyroid") were placed in each phantom. The central sections of the phantoms, used for dose determinations, were composed of polystyrene, a relatively expensive material with a CT density similar to water. The end sections of the phantoms were constructed of acrylic.

Resolving Power Module

A commonly used resolving power module was incorporated into one end of each of the phantoms (fig. 2). This module consists of nine parallel rows of holes drilled in the acrylic and filled with water. The diameters of the holes vary from 3.0 mm to 1.0 mm with 0.25 mm increments in hole diameter between rows. The holes in each row are the same size, and the distance between the centers of the holes is two times the hole diameter. The CT image of the resolving power module is shown in figure 3. The row of holes with the smallest diameter which could be clearly identified as distinct circles determined the resolving power of that CT scanner. The resolving power determination was made from the CT images of the module as they appeared on the cathode ray tube, but the images were also recorded on x-ray or Polaroid film. Radiographic factors for the resolving power determinations were the same as those used in the dose determinations and appear in the results section.

In order to calibrate the dependence of resolving power on dose for a given CT scanner, a series of scans were performed using the General Electric CT/T scanner and varying dose levels. All technical factors except tube current were held fixed. Using 288 1.1 msec pulses, scans were performed using tube currents of 40, 80, 160, and 250 mA, which corresponds to a range of 6.2:1 in dose.

Received November 15, 1977; accepted after revision March 24, 1978.
Presented at the annual meeting of the Society for Pediatric Radiology, Boston, September 1977.

[1] All authors: Department of Radiology, University of California School of Medicine, San Francisco, California 94143. Address reprint requests to R. C. Brasch.

0361-803X/78/0700-0095 $00.00

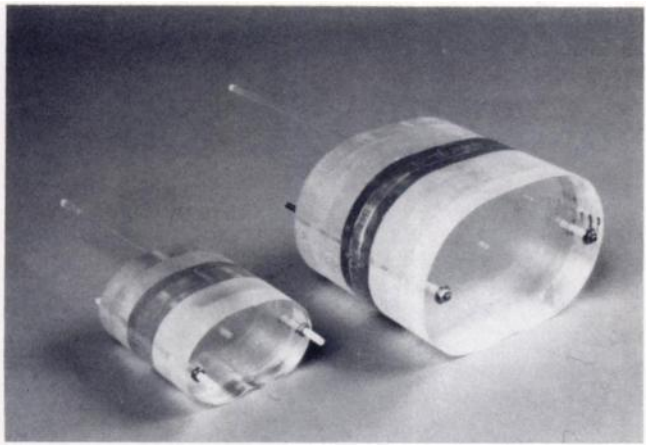

Fig. 1.—Two pediatric phantoms made in sections of acrylic and polystyrene (*center*) 36 and 66 cm in circumference. Each phantom was fitted with 10 thermoluminescent dosimeters, nine in plane of central section and one at end of plastic rod to simulate thyroid position.

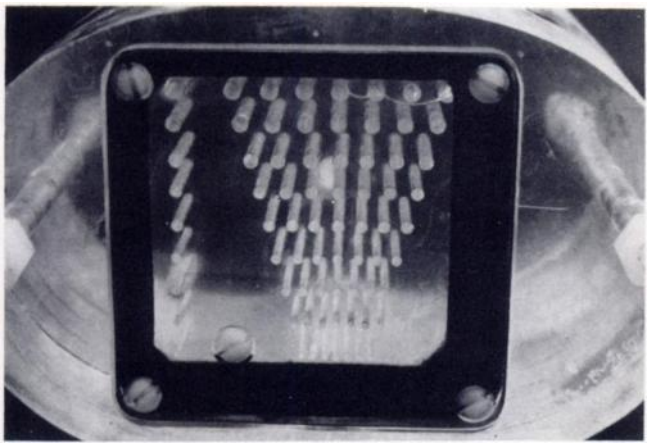

Fig. 2.—Close-up of resolving power module incorporated into each phantom. Rows of seven holes, filled with water, range in size from 3 mm in top row to 1 mm in bottom row. Holes change in size 0.25 mm between rows.

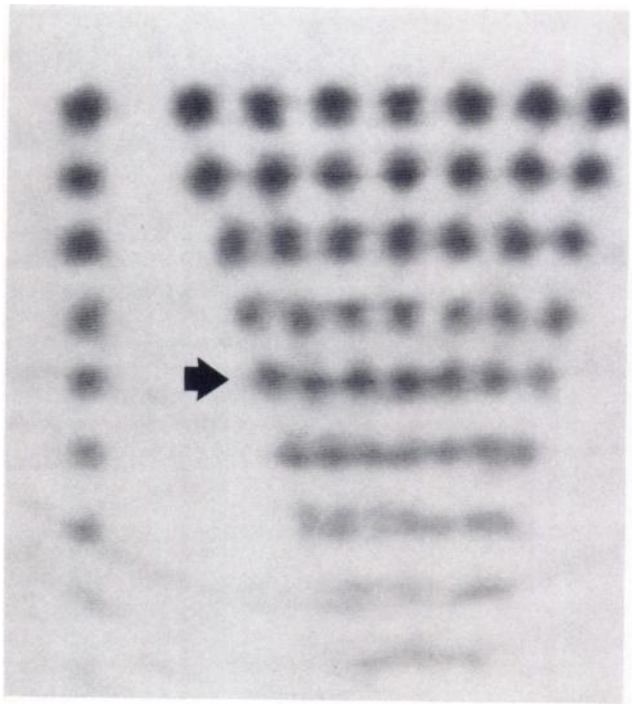

Fig. 3.—CT image of resolving power module. Holes in fifth row (*arrow*), 2.0 mm in diameter, are seen as distinct and separate circles. Holes in sixth row, 1.75 mm in diameter, are indistinct. Resolving power of this image is recorded as 2.0 mm.

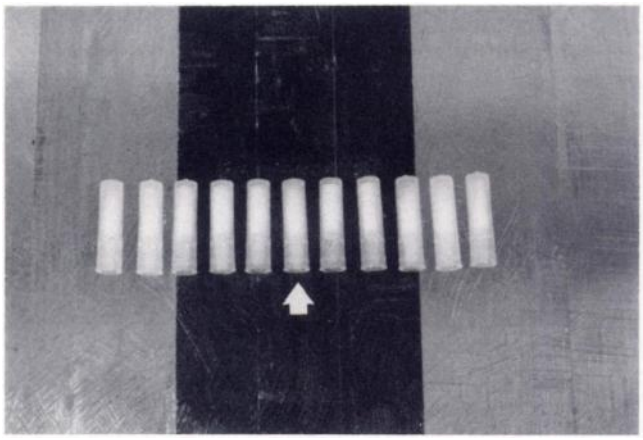

Fig. 4.—Arrangement of 11 thermoluminescent dosimeters across surface of phantom for determination of axial dose distribution. Dosimeters are aligned at 1 cm intervals and single CT section was directed at center dosimeter (*arrow*).

Dose Determinations

Radiation dose determinations were performed with both of the phantoms in each of the CT scanners with the exception of the Varian CT scanner in which only the larger phantom was used. The phantoms were loaded with thermoluminescent dosimeters for each determination and exposed to a series of eight consecutive CT sections. The phantom section containing nine of the dosimeters was in the center of the eight CT sections. The sections were at 1.0 cm intervals, except for the Ohio Nuclear Delta 50 fast scanner for which the interval was 1.3 cm. Every effort was made to simulate an actual CT examination of a pediatric abdomen. The radiographic factors were selected by the engineer or technician working with each CT unit as those factors "appropriate" for a child of similar size. Radiographic factors including tube potential, current, scanning mode, scanning circle, scanning time, and scanning interval are presented with the dosimetric data in the results section. For the EMI unit, bolus bags were packed around the circumference of the phantoms as is the practice for patients. No packing was used for the other CT scanners.

The average quadrant skin dose was calculated for each phantom and each CT unit by averaging the four circumferential surface doses in the central plane of the phantom.

Axial Dose Distribution

The axial distribution of radiation about a single tomographic section was determined for each CT scanner. Eleven thermoluminescent dosimeters were placed at 1 cm intervals in a row perpendicular to the tomographic section along the surface of the 66 cm phantom (fig. 4). The dosimeters were placed on the top of the phantom for all CT units except the Ohio Nuclear Delta 50, the Ohio Nuclear Delta 50 FS, and the Pfizer 200 FS models; for these three, they were placed on the undersurface of the phantom. These three scanners are designed so the x-ray

American Journal of Roentgenology 1978;131:95-101.

TABLE 1

Description of Surveyed Scanners

Scanner Model and Type	Location	Technical Factors			
		Degrees of Rotation*	Angle of Fan Beam (degrees)	Slice Thickness (mm)	Scanning Speed (sec)
Translate-rotate:					
EMI 5005	University of California, San Francisco	180	10	13	20
Pfizer 200 FS	Mt. Zion Hospital, San Francisco	270	20	10	28
Ohio Nuclear Delta 50	St. Francis Hospital, San Francisco	180	3	13†	69–153
Ohio Nuclear Delta 50 FS	Cleveland Clinic, Cleveland, Ohio	190	12	10	18
Rotary fan-rotary detector:					
General Electric CT/T	University of California, San Francisco	360	30	10	4.8
Varian	Stanford University, Palo Alto, California	360	. . .	10	3
Rotary fan-stationary detector:					
Ohio Nuclear Delta 2000 prototype	Cleveland Clinic, Cleveland, Ohio	360	. . .	10	2–16

Note – Testing dates are given in figs. 5 and 6.

* X-ray source moves above the body for the EMI 5005 and below the body for the Pfizer 200 FS and Ohio Nuclear Delta 50 and 50 FS.

† Two side-by-side 13 mm sections are performed simultaneously.

beam primarily comes from below, whereas the x-ray beam in the other models comes from above or moves 360° around the subject. The x-ray beam of a single tomographic section was directed through the central dosimeter in the array. The dose of radiation recorded by the dosimeters at progressively greater distances from the central one is a function of the beam collimation. Radiographic factors were the same as those used in the dosimetric determinations.

Scanners

Three types of commercial CT body scanners were included in the study as summarized in table 1. Technical descriptions of these scanner types have been published [1, 2]. Briefly, all types employ a fan beam of x-radiation in combination with a positron-sensitive detector array and various scanning motions. In the translate-rotate type, the fan beam and detector array rotate in angular increments about the body. At each angle the beam and detectors linearly traverse across the body. The rotary type scanners utilize a larger angle fan beam in order to cover the entire body section with a traversing motion. In rotating detector types, the detector array rotates opposite the beam through 360°. The stationary detector type utilizes a 360° fixed detector array of several hundred detectors so that only the x-ray source is required to rotate. The two rotating detector scanners studied use an array of pressurized Xenon gas ionization chambers which provide the necessary high gain stability. The other scanners use scintillation crystal-photomultiplier tube detectors.

All of the surveyed CT models have either 10 or 13 mm thick tomographic sections; the EMI 5005, Ohio Nuclear Delta 50, and the Ohio Nuclear Delta 50 fast scanner offer the greater widths. The Delta 50 scanner performs two side-by-side 13 mm sections simultaneously. Scanning speeds range from 3 to 153 sec with the rotary machines offering the faster speeds, an apparent advantage when scanning children. The Varian and General Electric scanners are pulsed x-ray sources; all others are continuous.

Results

The central section radiation doses for a series of eight consecutive scans are indicated in figures 5 and 6 for the 36 and 66 cm circumference phantoms, respectively. The technical factors of the scans including tube potential, tube current, pulse width (when applicable), scanning interval, scanning circle, and scanning speed as selected by the operator are indicated. Peak skin doses range from a high value of 8.0 rad for the EMI 5005 and the 36 cm phantom to a low of 0.49 rad observed for the same phantom with the General Electric CT/T scanner. Similarly, central internal doses range from 5.55 to 0.43 rad for these examples.

Table 2 summarizes the results of average quadrant skin dose and resolving power determinations for each scanner using the 66 cm phantom. Average quadrant skin doses for the larger phantom ranged from 0.45 rad to 4.30 rad, but the range in resolving power was relatively smaller, from 2.25 mm to 1.75 mm. Using the GE CT/T scanner, we found a two-thirds increase in dose (relative to the technique of fig. 6*B*) resulted in the ability to resolve the next smaller row of holes, a change in resolving power of 0.25 mm. Conversely, a two-thirds reduction in dose degraded the image so that the next larger row of holes was at the limit of resolution. Increments in dose less than 66% produced qualitatively observable differences in resolving power.

Figure 7 depicts the axial dose distributions for a single section at the peak skin dose region. In order to eliminate the effect of scatter, the upper bolus bag was removed in the EMI scanner, thus the results may be high by 20%–30% for this scanner. An attempt was made to align the sixth or middle dosimeter with the center of the scanned section. In the case of the Delta 50 FS and Delta 50 scanners, an error of 0.5 cm appeared and accordingly these curves were shifted along the axis to compensate. For purposes of illustration, all data points have been connected by straight line segments, although smooth curves, presumably Gaussian shaped, are expected. The full width at half maximum of these curves

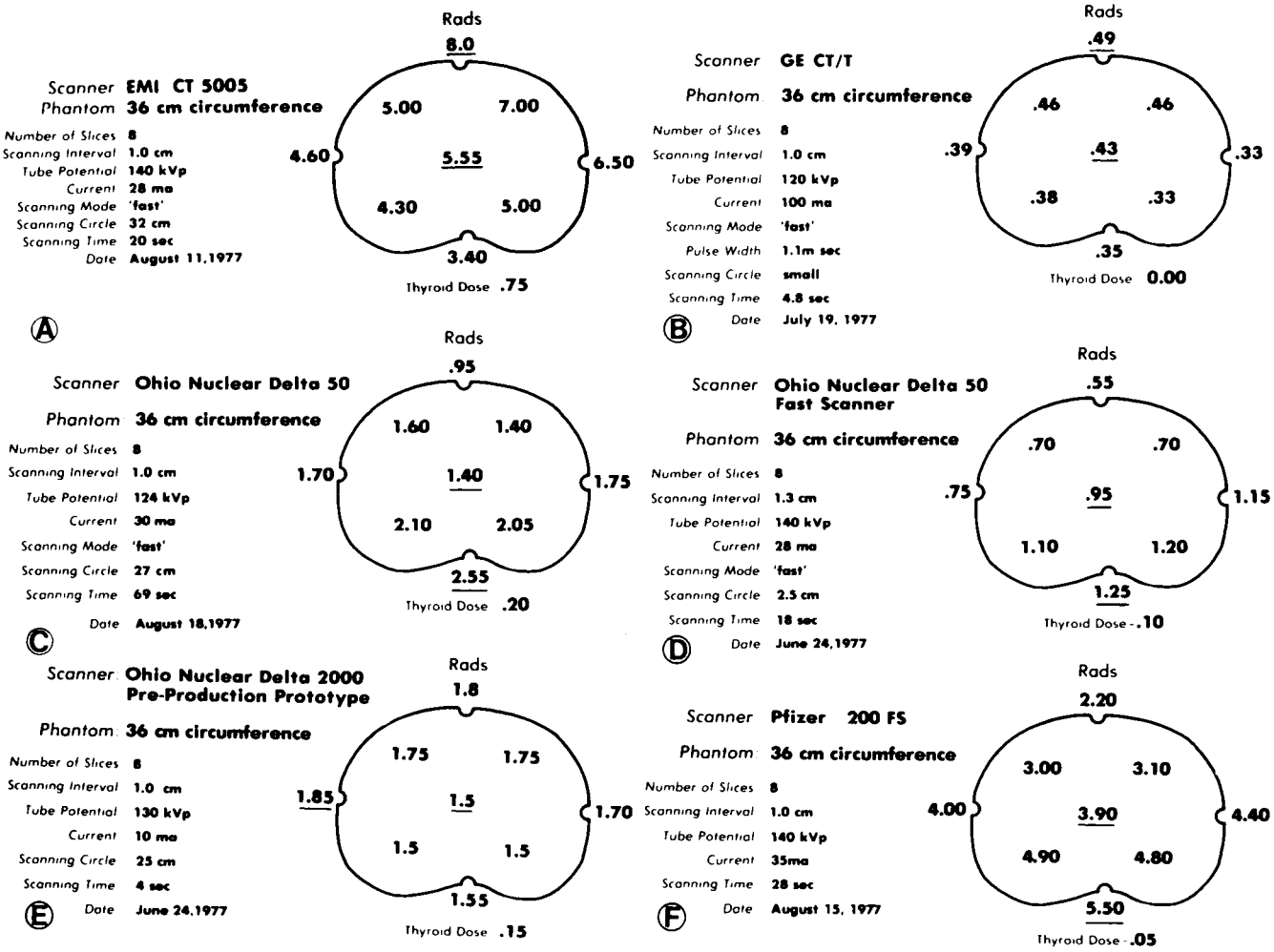

Fig. 5.—Results of radiation dose determinations with 36 cm phantom. All dose data except thyroid dose reflect radiation exposure in central plane of eight CT sections. Midplane and maximum skin doses are underlined.

ranges from 2.2 cm for the Ohio Nuclear Delta 50 scanner to 1.1 cm for the General Electric CT/T. The greater width of the Delta 50 scanner is a consequence of the fact that this unit performs two side-by-side 13 mm wide slices simultaneously.

Discussion

The axial dose distribution data of figure 7 can be used to estimate the cumulative dose from a series of scans at arbitrary intervals. The estimate can be formed by incrementing the axial distribution curve along the *X* axis according to the scan intervals and summating. For example, we may test our data for self-consistency by using the curves of figure 7 to predict the peak cumulated skin doses of figure 6 which were obtained from a series of eight scans at 1 or 1.3 cm steps. For example, the Pfizer 200 FS scanner single section axial radiation dose decreases to 33% of maximum at 1 cm from the central peak dose. Therefore, for a series of three scans at 1 cm steps we would expect the central cumulative dose to increase by a factor of 1.66 of the single section dose. Furthermore, the Pfizer single section dose decreases to 10% of maximum at 2 cm from the center, so that for five scans at 1 cm intervals we might predict a central peak skin dose of 1.86 times the single section dose of 2.15 rad, or approximately 4 rad. This estimate is a bit higher than the measured value of 3.3 rad from figure 6. A similar analysis for the General Electric axial dose distribution yields an estimate of 0.44 rad anterior skin dose compared to the measured value or 0.5 rad indicated in figure 6.

Several potential sources of small errors are present in our measurements. The dosimeters are measured by the commercial supplier with a reported precision of ±10%. Another factor, positioning of the phantom in the scanner, could introduce systematic errors due to the nonuniformity of the axial dose distributions for our eight scan studies. Peak doses tend to occur at the centers of the scanned sections with minimums in between. Specifically, for the Delta 50 scanner, Jucius and Kambic [3] have found a dose modulation of about 30% in the axial direction for multiple scans. This modulation would be larger for the scanners with the narrower single slice distributions. We estimate that such systematic errors

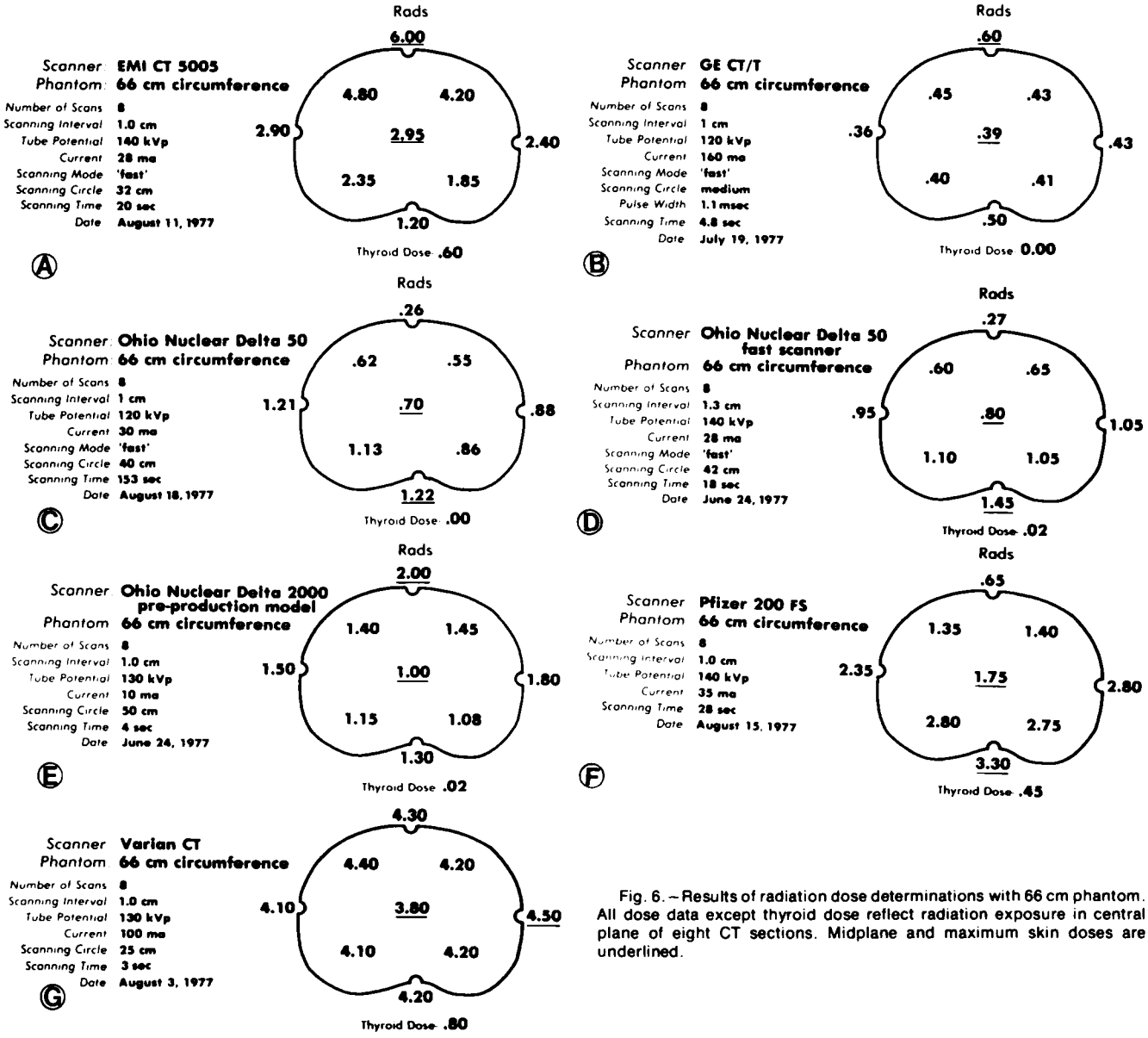

Fig. 6. – Results of radiation dose determinations with 66 cm phantom. All dose data except thyroid dose reflect radiation exposure in central plane of eight CT sections. Midplane and maximum skin doses are underlined.

are less than 20% for our study. Our results show good agreement with the findings of Jucius and Kambic [3] for the Delta 50 FS and with Yalcintas [4] who surveyed the EMI 5005.

In reviewing the data of figures 5–7, several interesting trends become apparent. The central and minimum skin doses tend to be larger for the smaller phantom of figure 5 than for the larger phantom of figure 6. This could be explained by relatively further penetration of the photon beam through the smaller phantom, yielding higher cumulative central and distal doses during the scan. An exception is the General Electric scanner which automatically selects lower tube current for smaller patients in order to maintain a constant number of detected photons. Potentially, similar adjustments could be made manually with other CT models.

The results summarized in figures 5–7 demonstrate a wide variation in absorbed dose among various scanners. We were interested in assessing the relationship of these dose variations to variations in image quality. The determination of image qualtiy in CT scanning is currently a controversial subject, and a complete, detailed survey of the imaging performance of CT scanners is beyond the scope of this paper. A detailed comparison of two of the surveyed scanners is presented by Boyd et al. [5].

Our simple resolving power test does evaluate one aspect of imaging performance at a specific contrast of 12%. This contrast corresponds approximately to the density difference between fat and soft tissue or soft tissue and bone, two common detection tasks in CT body scanning. At 12% contrast, objects of approxi-

TABLE 2
Skin Dose and Resolving Power

CT Model	Average Quadrant Skin Dose (rad)	Resolving Power (mm)*
General Electric CT/T	0.5 ± 0.1	2.25
Ohio Nuclear Delta 50 FS	1.0 ± 0.2	2.00
Ohio Nuclear Delta 50	1.8 ± 0.4	2.00
Pfizer 200 FS	2.3 ± 0.5	2.00
Ohio Nuclear Delta 2000 prototype	2.5 ± 0.6	1.75–2.00
EMI CT 5005	3.1 ± 0.6	2.25
Varian CT	4.3 ± 0.9	1.75

* Resolving power is measured with a 12% contrast (acrylic-water) phantom. For relationship of dose to resolving power at this contrast level, see text.

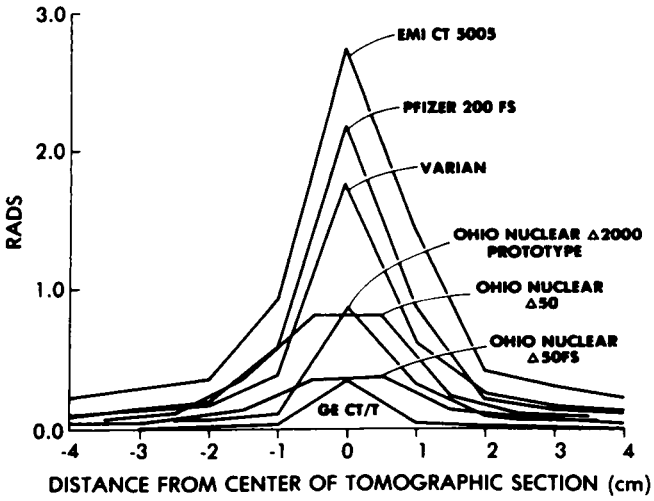

Fig. 7.—Axial dose distribution. Doses were recorded at 1.0 cm intervals from central, single CT section (0 on abscissa) for each of seven CT scanners. Curves can be used to estimate cumulative dose from series of scans at arbitrary intervals.

mately 2 mm in diameter can be resolved with all of the tested scanners. The observed contrast level with 2 mm water-filled holes in acrylic is typically lower than 12% by an amount that depends on the amount of blurring caused by spatial unsharpness. This decrease in effective contrast in small holes can be described mathematically by the modulation transfer function of each particular CT scanner. The ability to resolve nearby small holes depends on the relative magnitude of the image noise granularity [6] and the effective contrast of the holes. For a theoretical CT scanner with very fine sharpness, image contrast and object contrast would be the same, and resolving power would depend only on noise and, hence, dose. In this limiting case, it is possible to estimate the dependence of a resolving power test on dose. The noise in area elements of width W, $\sigma(W)$, may be described by the relationship

$$\sigma(W) = K(D^{1/2}/W^{3/2}),$$

where D is the absorbed dose and K is a constant [7]. Objects of size W can be resolved when the object contrast C is greater than $\sigma(W)$ by a small factor α [8]; that is, $\sigma(W)/C = \alpha$. Thus we may derive $(K/C)(D^{1/2}/W^{3/2}) = \alpha$ at the limiting resolution. Solving this equation, $D = (\alpha C/K)^2 W^3$. Thus a cubic relationship exists between resolving power W and dose D. This equation could be used to predict the dependence of resolving power on dose for a phantom constructed of large (greater than 2 mm) low contrast (less than 1%) holes. Such a phantom was not available to us at the time of the experiment. For our phantom, the effective contrast $C'(W)$ depends on the size of the holes and is lower than the object contrast, $C'(W) \leq C$. The relationship between dose and resolving power becomes

$$D = \alpha^2 \frac{[C'(W)]^2 W^3}{K^2}.$$

Since $C'(W)$ depends on the spatial sharpness of the CT scanner, our resolving power test reflects the spatial sharpness of a given scanner as well as its density resolution.

These factors combine to explain the relatively weak relationship between dose and resolving power observed using the GE scanner: a 0.25 mm decrease in W (about 10%) requires a two-thirds increase in dose, while a 0.25 mm increase in W requires a two-thirds decrease in dose. Referring to table 2, we see that this effect could be used to explain in part the observed wide variation in dose between different scanners, all of which differ only slightly in resolving power. For example, if the dose used by the GE scanner were increased by two-thirds by increasing the x-ray tube technique, resolving power would improve from 2.25 to 2.0 mm. Similarly, a large reduction in dose using the Varian scanner (threefold, if the dose-resolving power relationship for the GE scanner could be applied) would change the observed Varian resolving power from 1.75 to 2.0 mm. These factors would account for a great deal of the apparent difference in performance of these two scanners.

This discussion suggests the importance of selecting appropriate technical factors for a given CT examination. In cases where fine detail resolution is not required, it is possible to choose substantially lower levels of dose with only relatively small losses in image quality.

Some, but not all, of the variations summarized in table 2 can be explained by differences in image quality. Another important determinant of CT dose is the efficiency with which the scanner utilizes the x-ray photons that are directed through the body. Ideally, all transmitted photons would be detected and utilized by the image reconstruction processor. Many factors contribute to the inability of current CT scanners to achieve this goal. These include penumbra radiation falling outside the detectors in the axial direction, gaps between detectors, attenuators placed between patient and detectors, and low effective quantum efficiency of the detector system.

Axial penumbra radiation contributes to the broadening of the axial dose-distribution curve of figure 7; radiation falling outside of the effective tomographic section thickness is unused. CT scanners using point x-ray sources, such as the GE CT/T, can be more easily collimated to reduce out-of-plane penumbra radiation

than CT scanners using line sources. Gap width between detectors is an important problem for all three types of fan scanners, but this problem can be particularly significant in stationary detector array types where as much as 66% of the fan radiation may fall between detector elements. Bolus bags, as employed by the EMI-5005 scanner, also attenuate useful x-ray photons after passage through the body. The effective quantum efficiency of the detector system depends on both the energy spectral response of the detector and its photon-stopping efficiency, since integration techniques are used rather than counting methods. Gas detection systems present more difficult problems than solid scintillation systems in this respect. There seems to be a trend of increasing efficiency as manufacturers introduce newer models.

Benefit-Risk Analysis

Overall, the benefits of CT scanning in appropriately selected patients appear to outweigh the relatively small risks of this procedure. To assess the risk to pediatric patients, it is necessary to consider several factors in addition to the long term consequences of radiation exposure. Adverse reactions from the intravenous contrast media frequently used in CT examinations and the effects from other radiation-producing procedures accompanying the CT study (e.g., scout films) or eliminated by CT study must be considered.

Estimates of risk of death from radiation-induced cancer and leukemia are difficult to establish, particularly for pediatric subjects. However, based on analyses contained in works by Beir [9] and Unschar [10], the upper limits of risk for death by leukemia may be in the range of two per 100,000 patients exposed to 1 rad of whole body irradiation. Solid cancer deaths are approximately five times this rate. These admittedly high estimates of risk result in an estimate of total cancer deaths at one excess death per 12,500 patients studied by CT. This estimate assumes an average dose of 2 rad to one-third of the body. The actual risk of cancer-induced deaths from CT scanning may be considerably lower because assumptions were made that maximize the estimated risk.

Estimates of mortality from radiation-induced cancer must be integrated with the rare occurrence of idiosyncratic reactions to contrast media. The incidence of mortality in adults from intravenous contrast medium varies with different populations studied: one in 10,000 [11], one in 40,000 [12], and one in 75,000 [13]. However, severe reactions and death are relatively less common in pediatric populations [14], and not all CT patients receive contrast media.

An evaluation of risk from CT must also take into consideration the radiation dose from non-CT radiographic studies because CT can at times substitute for or suggest additional radiographic procedures. For example, CT images may eliminate the need for angiography. The maximum skin dose for an abdominal angiogram on a 10-year-old child has been determined to be 28.4 rad [15], a relatively high risk procedure with radiation exposure far exceeding that from CT. In such a situation, CT would be, in effect, a radiation-reducing procedure.

Considering the reported benefits of CT in children [16], the complex variables of risk, and evaluating a variety of CT devices, we believe that CT scanning in children is a relatively safe procedure with radiation exposures within the range of accepted, conventional radiographic techniques. As with all diagnostic radiologic procedures, the expected benefits must be weighed against the risks for the individual patient.

REFERENCES

1. Boyd D, Moss A, Korobkin M: Engineering status of computerized tomography. *SPIE Proceedings: Optical Instrumentation in Medicine* 96:303-321, 1976
2. Brooks RA, Di Chiro RA: Principles of computer assisted tomography. *Phys Med Biol* 21:689-732, 1976
3. Jucius RA, Kambic GX: Radiation dosimetry in computed tomography. *SPIE Proceedings: Optical Instrumentation in Medicine* 127:1-10, 1977
4. Yalcintas MG: Dose measurements with EMI 5005, technical report. Northbrook, Ill., EMI Medical, 1977
5. Boyd D, Margulis AR, Korobkin M: Comparison of translate-rotate and pure rotary CT body scanners. *SPIE Proceedings: Optical Instrumentation in Medicine* 127:280, 1977
6. Hansen K, Boyd D: The characteristics of reconstruction noise and their effect on detectability. *IEEE Trans Nucl Sci.* In press, 1978
7. Chesler DA, Riederer SJ, Pek NJ: Noise due to photon counting statistics in computed x-ray tomography. *J Comput Assist Tomogr* 1:64-74, 1977
8. Hansen K: Detectability in the presence of computed tomographic reconstruction noise. *SPIE Proceedings: Optical Instrumentation in Medicine* 127:304, 1977
9. Beir O: The effects on populations of exposure to low levels of ionizing radiation. Report of the Advisory Committee on the Biological Effects of Ionizing Radiation. Washington, DC, National Research Council, 1972
10. Unschar R: *Ionizing Radiation: Levels and Effects, Parts I and II,* A Report of the United Nations Scientific Committee on the Effects of Atomic Radiation to the General Assembly, Official Records of the General Assembly 27th session, suppl. 25 (A/8725), New York, United Nations, 1972
11. Shehadi WH: Adverse reactions to intravascularly administered contrast media. a comprehensive study based on a prospective study. *Am J Roentgenol* 124:145-152, 1975
12. Ansell G: Adverse reactions to contrast agents. Scope of the problem. *Invest Radiol* 5:374-384, 1970
13. Witten DM: Reactions to urographic contrast media. *JAMA* 231:974, 1975
14. Gooding CA, Berdon WE, Brodeur AE, Rowen M: Adverse reactions to intravenous pyelography in children. *Am J Roentgenol* 123:801-804, 1975
15. Webster EW, Alpert NM, Brownell GL: Radiation doses in pediatric nuclear medicine and diagnostic x-ray procedures, in *Pediatric Nuclear Medicine,* edited by James AE, Wagner HM Jr, Cooke RE, Philadelphia, Saunders, 1974, pp 34-58
16. Brasch RC, Korobkin M, Gooding CA: Computed body tomography in children: evaluation of 45 patients. *Am J Roentgenol* 131:21-25, 1978

American Journal of Roentgenology 1978.131:95-101.